Seasonal variations measured by TDR and GPR on an anthropogenic sandy soil and the implications for utility detection

Curioni, Giulio; Chapman, David; Metje, Nicole

DOI:
10.1016/j.jappgeo.2017.01.029

Document Version
Publisher's PDF, also known as Version of record

Citation for published version (Harvard):
Curioni, G, Chapman, D & Metje, N 2017, 'Seasonal variations measured by TDR and GPR on an anthropogenic sandy soil and the implications for utility detection', *Journal of Applied Geophysics*, vol. 141, pp. 34-46. https://doi.org/10.1016/j.jappgeo.2017.01.029

Journal of Applied Geophysics 141 (2017) 34–46

Contents lists available at ScienceDirect

Journal of Applied Geophysics

journal homepage: www.elsevier.com/locate/jappgeo

Seasonal variations measured by TDR and GPR on an anthropogenic sandy soil and the implications for utility detection

Giulio Curioni *, David N. Chapman, Nicole Metje

School of Engineering, Department of Civil Engineering, University of Birmingham, Edgbaston, Birmingham B15 2TT, United Kingdom

ARTICLE INFO

Article history:
Received 26 July 2016
Received in revised form 7 December 2016
Accepted 24 January 2017
Available online 25 January 2017

Keywords:
Seasonal electromagnetic soil properties
Time Domain Reflectometry
Ground Penetrating Radar
Field monitoring
Geophysics
Utility detection

ABSTRACT

The electromagnetic (EM) soil properties are dynamic variables that can change considerably over time, and they fundamentally affect the performance of Ground Penetrating Radar (GPR). However, long-term field studies are remarkably rare and records of the EM soil properties and their seasonal variation are largely absent from the literature. This research explores the extent of the seasonal variation of the apparent permittivity (K_a) and bulk electrical conductivity (*BEC*) measured by Time Domain Reflectometry (TDR) and their impact on GPR results, with a particularly important application to utility detection. A bespoke TDR field monitoring station was specifically developed and installed in an anthropogenic sandy soil in the UK for 22 months. The relationship between the temporal variation of the EM soil properties and GPR performance has been qualitatively assessed, highlighting notably degradation of the GPR images during wet periods and a few days after significant rainfall events following dry periods. Significantly, it was shown that by assuming arbitrary average values (i.e. not extreme values) of K_a and *BEC* which do not often reflect the typical conditions of the soil, it can lead to significant inaccuracies in the estimation of the depth of buried targets, with errors potentially up to approximately 30% even over a depth of 0.50 m (where GPR is expected to be most accurate). It is therefore recommended to measure or assess the soil conditions during GPR surveys, and if this is not possible to use typical wet and dry K_a values reported in the literature for the soil expected at the site, to improve confidence in estimations of target depths.

1. Introduction

The goal of remote sensing of the subsurface, particularly in urban environments, is to create an accurate 3D representation of the ground and all other buried features. For streetworks operations, this activity becomes crucial as an accurate knowledge of the subsurface allows appropriate planning for quick and clean operations, with minimal impacts on traffic, businesses and multiple other city disruptions under all three pillars of sustainability (Read and Vickridge, 2004; Rogers, 2015). With increasing demands on surface space in cities, more and more attention is been given to the use of underground space (Bobylev, 2016). Ground Penetrating Radar (GPR) and other remote sensing technologies are often reliable creators of 2D maps, but accurate depth estimations remain a major challenge, which is recognised by the ASCE (2002) guidelines, which do not attribute depth information to geophysical survey data in contrast to the BSI (2014) specification. Inaccurate depth information can have significant consequences ranging from increased risk of utility strikes (Metje et al., 2015) to requiring trench wall support for deeper excavations. As a result, operators and the public's health and safety are at risk, as well as delays to the project if site operations are not prepared for any complications resulting in significant added costs. In addition, in urban areas in particular, the subsurface is very congested and complicated with services of different ages and at different depths therefore accurate location including depth is vital (Fig. 1).

More generally, GPR is employed in a wide variety of applications, such as the identification of soil layers, the depth of shallow bedrock and the water table, the detection of land mines, the location of utilities and the identification of archaeology just to mention a few, but for all of these depth information is absolutely vital (Daniels, 2004). However, the ability of GPR to detect underground features is strongly dependent on the electromagnetic (EM) properties of the soil, which are affected by the soil type and conditions (Doolittle and Collins, 1995; Doolittle et al., 2007). Comprehensive characterisation of the EM behaviour of soils is essential when applying shallow geophysical methods such as GPR for investigating the subsurface if the ambitious goals of accurate 3D mapping are to be achieved. This paper represents the culmination of a novel and ambitious programme of research to make a step change in the understanding of the soil EM properties for surface remote surveying of the subsurface (Thomas et al., 2008, 2010a, 2010b; Thring et al., 2014).

* Corresponding author.
E-mail address: g.curioni@bham.ac.uk (G. Curioni).

http://dx.doi.org/10.1016/j.jappgeo.2017.01.029

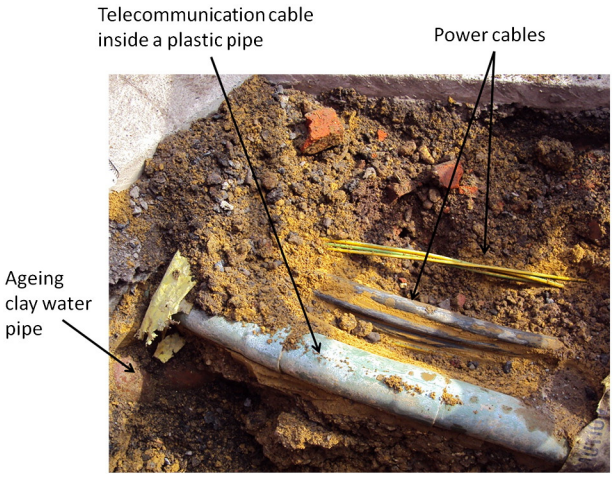

Fig. 1. Example of service utilities commonly found in urban areas.

Therefore, a significantly increased understanding of the variation of the EM soil parameters with different soil properties and more importantly with weather conditions, in particular water infiltration, is vital to improve the depth resolution of GPR and other geophysical survey technologies (Foo et al., 2011; Rogers et al., 2009), allowing for better planning and interpretation of surveys. A direct knowledge of the variability of the soil's EM properties encountered in the field will give GPR practitioners the tools necessary for selecting the best equipment, providing better confidence in the data (including depth) and ultimately leading to an improved 3D representation of the subsurface, which has significant benefits to their clients.

The fundamental EM soil properties are the dielectric permittivity, the electrical conductivity and the magnetic permeability. Soils are often considered non-magnetic (Cassidy, 2009), although this is not true if they contain significant amounts of magnetic minerals such as iron oxides (Cassidy, 2008). The EM behaviour of non-magnetic soils can be described by the electrical properties only (i.e. dielectric relative permittivity and electrical conductivity).

Several techniques, including GPR and Time Domain Reflectometry (TDR), have been successfully used to estimate the soil water content based on the measurement of the EM soil properties (Huisman et al., 2003a; Robinson et al., 2003; Topp et al., 1980). More recently it has been shown that these properties are related to basic geotechnical parameters, such as the Atterberg limits and the linear shrinkage which could potentially be used for their prediction (Rogers et al., 2009; Thomas et al., 2010a, 2010b). This would be a significant advantage to geotechnical engineers and geophysicists as it is often easier to determine the geotechnical soil properties in the field. This would also benefit all geophysical surveys relying on EM signal transmission with applications ranging from buried utilities to mineshafts and archaeology.

Past research involving EM sensors such as TDR has primarily focussed on the measurement of the soil water content based on the apparent permittivity (K_a) and, in some cases, on the bulk electrical conductivity (*BEC*, S/m) (Bittelli et al., 2008, Heimovaara and Bouten, 1990, Herkelrath et al., 1991, Herkelrath and Delin, 2001, Logsdon, 2005). TDR has the advantage to be able to measure both parameters, although not all the available commercial systems offer this possibility (Robinson et al., 2003). Field measurements by TDR have successfully been carried out in the past (Herkelrath et al., 1991, Herkelrath and Delin, 2001; Menziani et al., 2003, Rajkai and Ryden, 1992). However, the simultaneous and continuous long-term field monitoring of both K_a and *BEC* is starkly noticeable by its absence in the literature. Long-term (i.e. seasonal) field monitoring of the EM soil properties has considerable benefits when compared with repeated GPR measurements as it would provide a comprehensive understanding of the soil behaviour and useful insights on the use of the GPR technique. The key benefit of TDR is that it operates on similar principles to GPR and hence is particularly well suited for supplementing GPR data during monitoring applications as it can provide more detailed insights on the spatial and temporal variations of the soil properties. Both TDR and GPR work at a similar frequency range (i.e. approximately 10 MHz to 1 GHz) and therefore the two techniques can be directly compared and used effectively in combination. In this frequency range the measurements respond predominantly to the amount of free water within the soil and are less affected by the bound water held on the surface of the soil particles (Saarenketo, 1998; Gong et al., 2003). The total water content (i.e. bound and free water) of the soil can be measured with alternative techniques such as neutron probes and nuclear magnetic resonance sensors although they are currently not commonly used due to high cost and health and safety issues. Other widely used EM techniques such as the capacitance probes and electrical resistivity methods operate at a lower frequency range and therefore are less comparable to GPR. They are also more susceptible to temperature variations, salinity and soil texture than TDR (Robinson et al., 2003). The main difference between TDR and GPR is the sampling volume, with TDR measuring a small volume of a few cm^3 around the probe (Ferré et al., 1998) while GPR measures a greater volume of the order of several m^3, depending on the equipment used and the attenuation of the soil. Previous studies compared point measurements from TDR sensors and GPR measurements using the ground wave propagating through the topsoil (Huisman et al., 2001, 2003b). However, due to the limited penetration depth of the ground wave, these studies investigated only a shallow depth of a few centimetres below the surface. Weiler et al. (1998) used TDR probes at different depths to establish a soil specific calibration and compared the results to GPR measurements. However, TDR sensors were not left long-term on site and a discussion on the seasonal effects on the GPR performance was not carried out.

The seasonal variation of soil properties has been investigated in the past in order to understand their effect on the GPR ability to detect soil layers (Boll et al., 1996; Kowalsky et al., 2001; Lunt et al., 2005; Zhang et al., 2014). However, these studies discussed only the results of selected field campaigns not repeated over the years, possibly failing to account for more rare extreme conditions. The literature provides no information of studies conducted in the field of utility detection combined with the influence of changing soil conditions on the depth estimates of the targets. As highlighted previously, if this information is not accurate in the 3D representation of the buried assets in the ground, it can lead to a significantly increase in health and safety risks and cost due to additional traffic congestion, project delays and utility damage.

The aim of this paper therefore is to fill a gap in the literature with respect to long term monitoring of K_a and *BEC* using TDR and relating this to GPR surveys for utility detection throughout a range of weather conditions. Both short-term (i.e. daily) and long-term (i.e. seasonal) variations were investigated and quantified by a bespoke TDR installation and their influence on GPR surveys for buried utility detection assessed. An analysis of the potential errors in depth estimates induced by changing soil properties, vitally significant for accurate 3D models, is also presented.

2. Electromagnetic monitoring with TDR and GPR

TDR and GPR are both EM methods working on analogous principles and are similarly dependent on the EM properties of the soil, i.e. the dielectric permittivity, the electrical conductivity and the magnetic permeability.

The dielectric permittivity is a measure of the ability of a material to polarise under the influence of an electric field. It represents the signal energy that can be stored in a material through separation of charges. It is described by a frequency dependent complex number, $\varepsilon_r^*(f)$, with the real part representing the storage of energy, $\varepsilon_r'(f)$, and the imaginary part describing the loss mechanisms, $\varepsilon_r''(f)$. It is normally expressed

as the ratio to the dielectric permittivity of free space (ε_0, 8.854 × 10^{-12} F/m). The relative complex dielectric permittivity, $\varepsilon_r^*(f)$ – from now on the terms 'relative' and 'dielectric' will be omitted – is given in Eq. (1).

$$\varepsilon_r^*(f) = \varepsilon_r'(f) - j\left(\varepsilon_p''(f) + \frac{\sigma_{dc}}{2\pi f \varepsilon_0}\right) \quad (1)$$

where $\varepsilon_p''(f)$ represents the dipolar losses due to relaxation, σ_{dc} is the static electrical conductivity (S/m), f is the frequency (Hz) and j is the imaginary number, $\sqrt{-1}$. TDR measures an apparent permittivity that comprises both the real and imaginary parts of the complex permittivity and can be approximated to the real permittivity only in low-loss materials (Bittelli et al., 2008; Topp et al., 2000). The soil apparent permittivity, K_a (note that the symbols ε and K have been used interchangeably in the literature, see for example Robinson et al., 2003 and Huisman et al., 2003a), is defined by Eq. (2).

$$K_a = \frac{\varepsilon_r'(f)\mu_r}{2}\left(1 + \sqrt{1 + \left(\frac{\varepsilon_p''(f) + \frac{\sigma_{dc}}{2\pi f \varepsilon_0}}{\varepsilon_r'(f)}\right)^2}\right) \quad (2)$$

where μ_r is the relative magnetic permeability, expressed as the ratio between the absolute magnetic permeability of the soil and the absolute magnetic permeability of free space (μ_0, 1.26 × 10^{-6}H/m). For low-loss soils K_a is related to the signal propagation velocity, v (m/s), by Eq. (3).

$$v = \frac{c}{\sqrt{K_a}} \quad (3)$$

where c is the speed of light in a vacuum (2.9979 × 10^8 m/s).

The principle on which TDR operates is similar to the principle of radar. TDR sends a broadband EM pulse into a coaxial transmission line comprising a cable and a probe, usually consisting of two or three metal rods, and measures the reflections resulting from an impedance change (Robinson et al., 2003). The frequency corresponding to the measured K_a (Eq. (2)) depends on the equipment used and on the dispersive nature of the soil (i.e. the variation of the complex permittivity with frequency), and is generally not easily specified (Robinson et al., 2003). The typical TDR frequency bandwidth is between 10 MHz and 1 GHz (Topp et al., 2000). According to Eq. (2) the soil K_a includes the magnetic characteristics, together with the dielectric losses due to relaxation and electrical conductivity. However, practical geophysical applications such as GPR do not necessarily require knowledge of each individual component and K_a is most useful because of its relationship with the signal propagation velocity (Eq. (3)). In addition, TDR is able to measure the low frequency value of *BEC* that is reasonably close to the static conductivity (Topp et al., 2000) and gives an indication of the signal attenuation. Therefore TDR can be used to characterise the EM behaviour of soils. Extensive information on the calibration and measurement of K_a and *BEC* by TDR are found in the literature and are not discussed here (see, among others, Bechtold et al., 2010, Curioni et al., 2012, Lin et al., 2007, 2008, Huisman et al., 2008, Robinson et al., 2003).

GPR can be used to measure the soil K_a in the presence of a clear target (Huisman et al., 2003a). In the case of linear buried utilities such as pipes, the typical GPR response taken from transects perpendicular to the target is a hyperbola. The average K_a of the soil above the target can be measured by fitting the hyperbola (Huisman et al., 2003a), from which the signal velocity can be calculated using Eq. (3) and the depth of the target estimated. Conventionally, GPR has the disadvantage that it cannot be automated for field surveys and therefore is less suited for continuous monitoring.

3. Field case study

3.1. Site characterisation

A TDR-based field monitoring station was developed at the University of Birmingham campus (UK) in order to continuously monitor the soil K_a and *BEC* for a long-time period covering different seasons (Curioni, 2013). The test site was located on quaternary glaciofluvial deposits dated to the Middle Pleistocene (0.126–0.781 Ma). The water table was known to vary between 6.5 m and 8.0 m depth (Hatzichristodulu et al., 2002). According to BSI (2015) the investigated soil was very gravelly SAND comprising a topsoil of 0.20 m overlaying a sandy subsoil. For convenience of analysis, the subsoil was divided into subsoil 1, from approximately 0.20 and 0.70 m, and subsoil 2, from 0.70 and 1.10 m, with slightly higher clay content (Fig. 2a). Aside from its easily accessible location, the site was chosen because was deemed to be relatively representative of urban environments. In fact, the soil lacked specific structure, it contained anthropogenic materials such as bricks and traces of coal, and was disturbed during construction works that occurred a few decades ago. Furthermore, although the soil was not covered with a hard surface, it was deemed representative of urban conditions as it was rich in sand, gravel and cobbles, materials typically found under roads and pavements. Moreover, it represents anthropogenic fill which is common in urban environments where the parent soil has been displaced during development processes. According to the British Geological Survey superficial geology map (BGS 1:50,000) similar sand and gravel deposits are widespread in the UK and found in several major urban areas.

The characterising parameters for the three horizons are summarised in Table 1. Density and oven-dried gravimetric water content (GWC) were measured on samples collected before the TDR installation. Due to the limited depth of the manual excavation the density and GWC were not measured for the deeper horizon. pH and organic matter (OM) were measured from samples taken during the TDR field installation.

3.2. Field monitoring

The monitoring equipment consisted of a Campbell Scientific TDR100 device, three SDMX50SP multiplexers and two arrays of eight CS645 TDR probes (three-rod, 75 mm long, 3 m cable length) installed horizontally down to approximately 1 m depth and 1 to 2 m apart (Fig. 2b). The reason for using two arrays derived from the need for cross-validation of the results and also as a backup in the event of probe failure. Three temperature sensors were also buried at different depths. The TDR probes were relatively shallow in order to provide detailed information on the typical depth of utilities in the UK (Thomas et al., 2009). Measurements were taken with hourly frequency for a period of approximately 22 months, starting the 20th August 2010 and ending the 6th July 2012. A number of gaps in the data occurred during this period mainly related to problems with the power supply. Further details on the experimental development, calibration and data processing are reported in Curioni et al. (2012) and Curioni (2013). The measurement error of the TDR setup used in this study was shown to be ±2% and ±3% for K_a and *BEC*, respectively, based on travel time measurements in liquids. Weather data were collected from a weather station located approximately 100 m from the test site. In addition to the continuous monitoring by TDR, regular GPR surveys (approximately once a week) were conducted on a predefined transect over specifically buried targets in order to study the impact of the temporal variations of the EM soil properties on GPR (Fig. 2c and d). The targets were 25 mm diameter stainless steel pipes and 100 mm diameter (air-filled and sealed at both ends) plastic pipes, 2.5 m and 2 m long, respectively, and were buried at different depths down to approximately 1 m. The Detector Duo GPR system by IDS (Ingegneria Dei Sistemi) was used giving an output frequency at approximately 250 MHz and 700 MHz. A standard processing technique included in the GRED software provided by the GPR manufacturer was

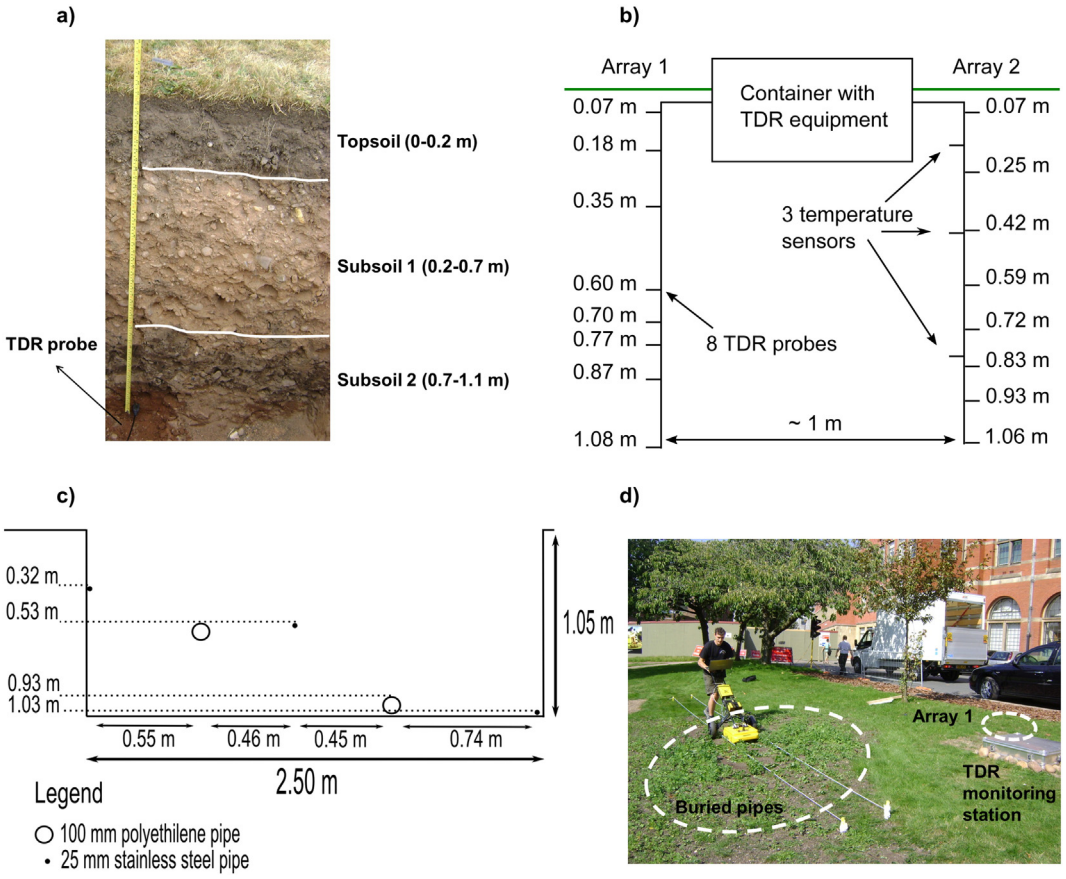

Fig. 2. a) Test site soil profile, b) schematic diagram of the TDR installation, c) vertical cross-section of the buried targets, d) predefined GPR transect perpendicular to the buried pipes and positioned next to the TDR monitoring station.

used to analyse the data and involved vertical and horizontal bandpass filters, smoothed gain and moved start time (i.e. zero time correction). The identified hyperbolae were manually fitted using the GRED software in order to calculate the average K_a of the soil above the target (Huisman et al., 2003a). In order to reduce uncertainty in the analysis, the mean values obtained from four repeated scans along the same transect were used. The differences between different scans were found to be negligible.

4. Results and discussion

4.1. Seasonal variation of the EM soil properties

During the monitoring period the soil EM properties varied significantly, which has a significant impact on the interpretation of geophysical survey data. Fig. 3 shows the variation with depth of K_a and *BEC* measured by each TDR probe and for both arrays. The variability with depth decreased during dry conditions, expressed by minima values of EM soil properties. Conversely, a higher variability with depth was measured during wet periods. In this case, higher values of the EM soil properties were measured by the shallower probes inserted in the topsoil and by the deeper probes inserted in the more clayey soil horizon. This variability within the soil profile can lead to multiple reflections and hence contribute to the degradation of the GPR results (see later Section 4.3). Fig. 3 demonstrates the existence of similar trends for both arrays, although the absolute values were not always consistent.

The summary statistics of the measured properties organised by soil horizon for the entire period of field monitoring are shown in Table 2. The extent of variation occurring in the soil studied was significant, with K_a changing over a factor of 7 for the topsoil and 3 for the subsoil. The corresponding propagation velocity calculated from Eq. (3) varied by a factor of approximately 3 and 2 for the topsoil and subsoil, respectively. The magnitude of *BEC* changed by a factor of more than 100 for the topsoil and 8 for the subsoil, however the values remained low over the monitored period due to the sandy nature of the soil. Despite the seasonal variation of *BEC* being less significant for this soil, the change in K_a has important implications for the transmission of EM waves through soil. Examples of GPR results taken at extreme conditions are described later and demonstrate the importance of this variation.

In order to determine the depth of buried targets the propagation velocity of GPR signals must be known and can be calculated from a measurement or estimation of the soil K_a according to Eq. (3) (Martinez and Byrnes, 2001; Pennock et al., 2012). Typical ranges of values for different materials are reported in the literature, often with a distinction between wet and dry conditions (Daniels, 2004). It is crucial to note that mean

Table 1
Characterisation of the investigated soil at the University of Birmingham test site. [Note: the particle size percentages are by weight and were calculated according to BSI (1999).]

Depth (m)	Gravel (%)	Sand (%)	Silt + clay (%)
0.00–0.20	1	87	12
0.20–0.70	48	48	4
0.70–1.10	34	57	9

Depth (m)	ρ_{dry} (g/cm^3)	ρ_{bulk} (g/cm^3)	ρ_{part} (g/cm^3)	GWC (%)
0.00–0.20	1.11	1.50	–	35.87
0.20–0.70	1.49	1.67	2.66	12.50

Depth (m)	pH	OM (%)
0.00–0.20	5.94	4.7
0.20–0.70	6.35	0.9
0.70–1.10	6.30	1.3

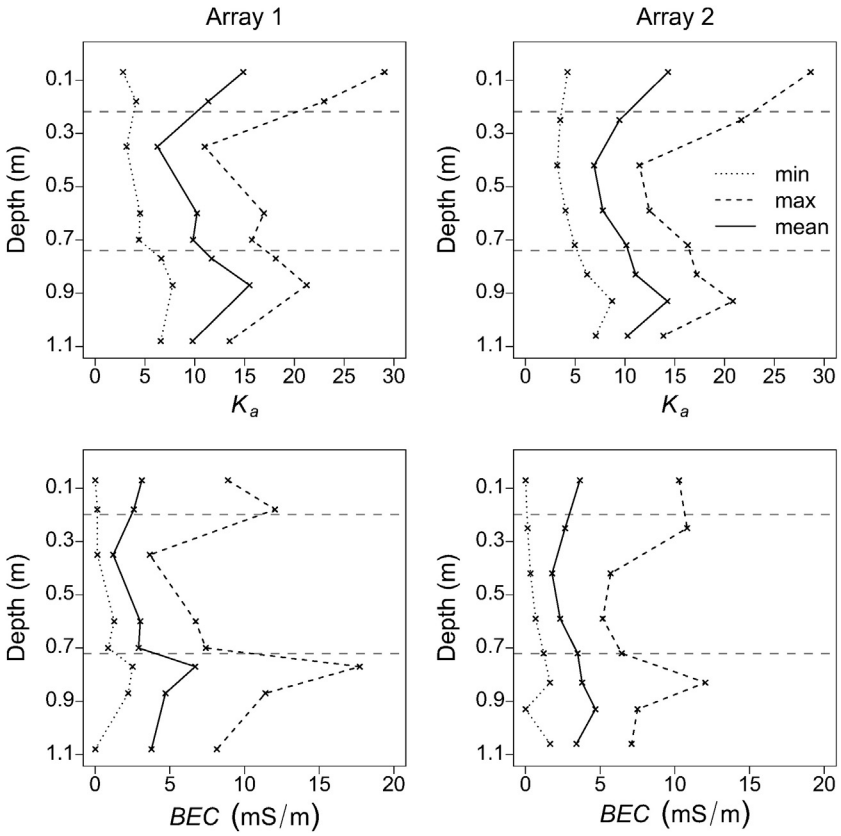

Fig. 3. Variability with depth of the soil K_a and *BEC* measured by the TDR probes for each array during the entire field monitoring. [Note: the horizontal lines show the approximate position of the soil horizons; the markers indicate the depth of the TDR probes.]

Table 2
Summary statistics of the measured soil properties by soil horizon.

	K_a			*BEC* (mS/m)			Temperature (°C)			Velocity (m/ns)		
	Min	Max	Mean	Min	Max	Mean	Min	Max	Mean	Min	Max	Mean
Topsoil	3.7	25.6	12.5	0.1	10.5	3.0	2.0	21.1	10.1	0.059	0.157	0.085
Subsoil 1	4.0	14.0	8.5	0.8	5.9	2.5	3.0	20.0	12.4	0.080	0.149	0.103
Subsoil 2	7.2	17.5	12.1	1.3	10.7	4.5	2.0	21.4	12.2	0.072	0.112	0.086

values are likely not representative of the real soil conditions. For this case study this is demonstrated by the frequency histograms shown in Fig. 4. It is apparent that K_a and *BEC* were not normally distributed and two approximate peaks could be identified corresponding to dry and wet conditions (i.e. low and high values, respectively). In particular, the mean K_a values did not occur often during this period and extreme values were more common. During the monitored period extreme conditions occurred (Spring 2011 was very dry, Spring 2012 was very wet) and this allowed the full range of the EM properties of the soil studied to be measured. It is worth noting that these extreme conditions were sampled only thanks to the continuous long-term monitoring programme covering multiple seasons over two consecutive years.

Fig. 5 shows the seasonal variation of the rainfall, air temperature and of the EM soil properties for each horizon during the monitoring period. The data correspond to the daily rainfall, the daily air temperature and the daily means of all the probes inserted in each soil horizon. The topsoil showed greater seasonal variability, with the largest difference between the maxima and minima values. Because of the direct influence of rainfall and evaporation events, a higher variability was also visible for the topsoil over shorter periods of time. Similar dynamics were reported by other authors for soil water content (Menziani et al., 2003; Rajeev et al., 2012). Both subsoil horizons, which only contained small amounts of clay and therefore had low water holding capacity, showed more homogeneous values. K_a varied significantly, with higher values in Winter and lower values in Summer.[1] *BEC* followed a similar trend but showed a smaller variation because of the sandy and gravelly nature of the soil studied. Fig. 5 indicates the existence of a positive relationship between the EM soil properties and rainfall and an approximate inverse relationship with air temperature over the Summer months.

4.2. Short-term variation of the EM soil properties

One of the benefits of a continuous soil monitoring station is the ability to study short-term changes in the soil conditions, including diurnal variations and the effect of precipitation events. Fig. 6 shows the variation of the EM soil properties for two selected periods occurring in Spring 2011, during dry conditions, and in Spring 2012, during wet conditions, respectively. In both cases the soil temperature did not vary significantly, with differences between maxima and minima smaller than 3 °C despite a change in the air temperature of more than 8 °C over a 24 h period. Both K_a and *BEC* remained approximately constant during the selected periods and changed noticeably only corresponding

[1] The seasons by calendar were defined as follows. Winter: Dec 21–Mar 20, Spring: Mar 21–Jun 20, Summer: Jun 21–Sep 22, Autumn: Sep 23–Dec 20.

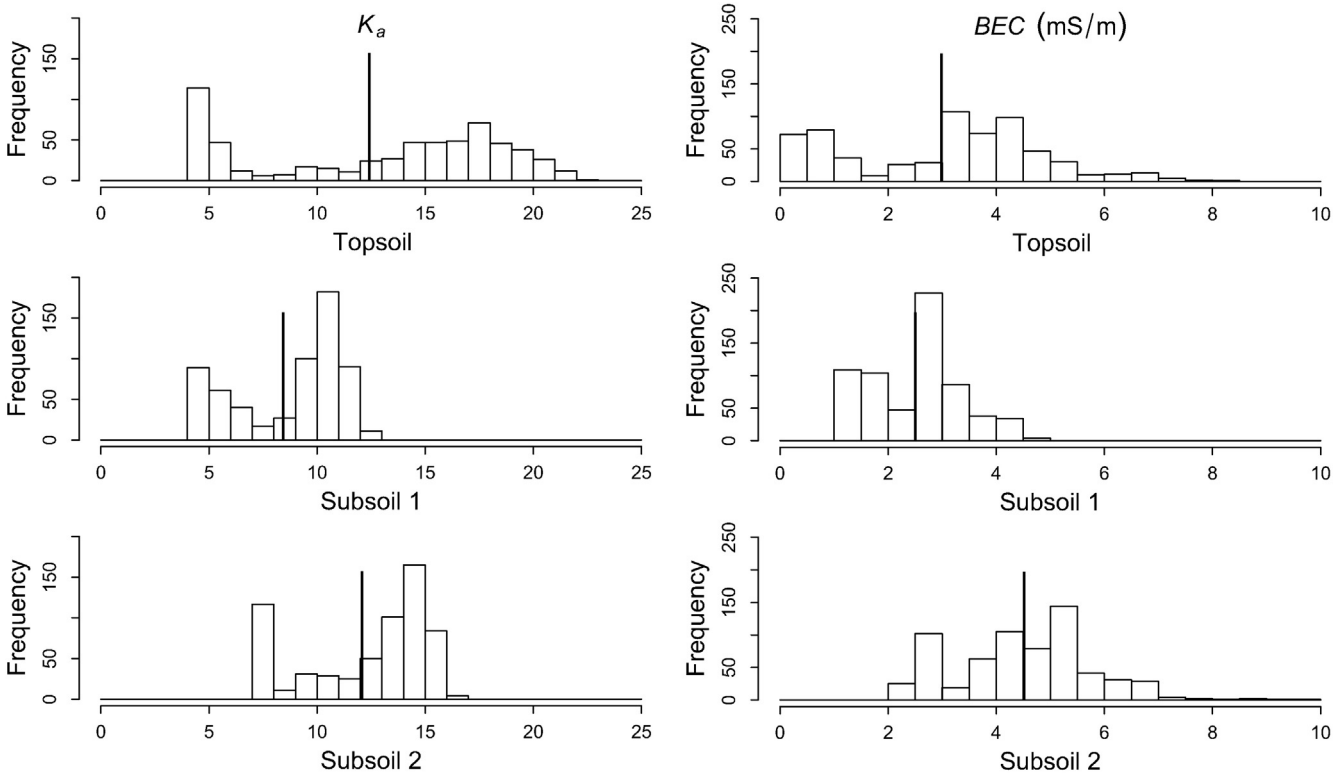

Fig. 4. Frequency histograms of the measured K_a and *BEC* by soil horizon. [Note: the vertical lines indicate the mean values recorded during the monitoring period.]

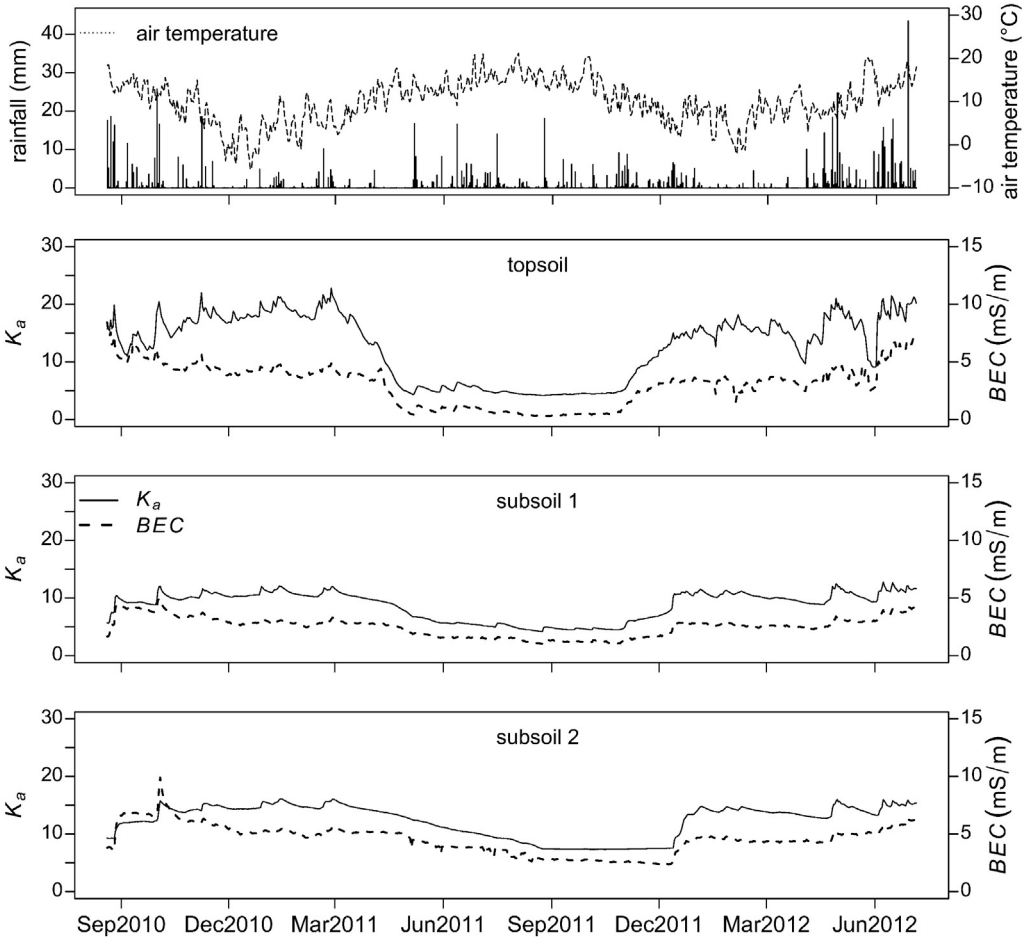

Fig. 5. Temporal variation of the daily rainfall, air temperature, K_a and *BEC* for each soil horizon.

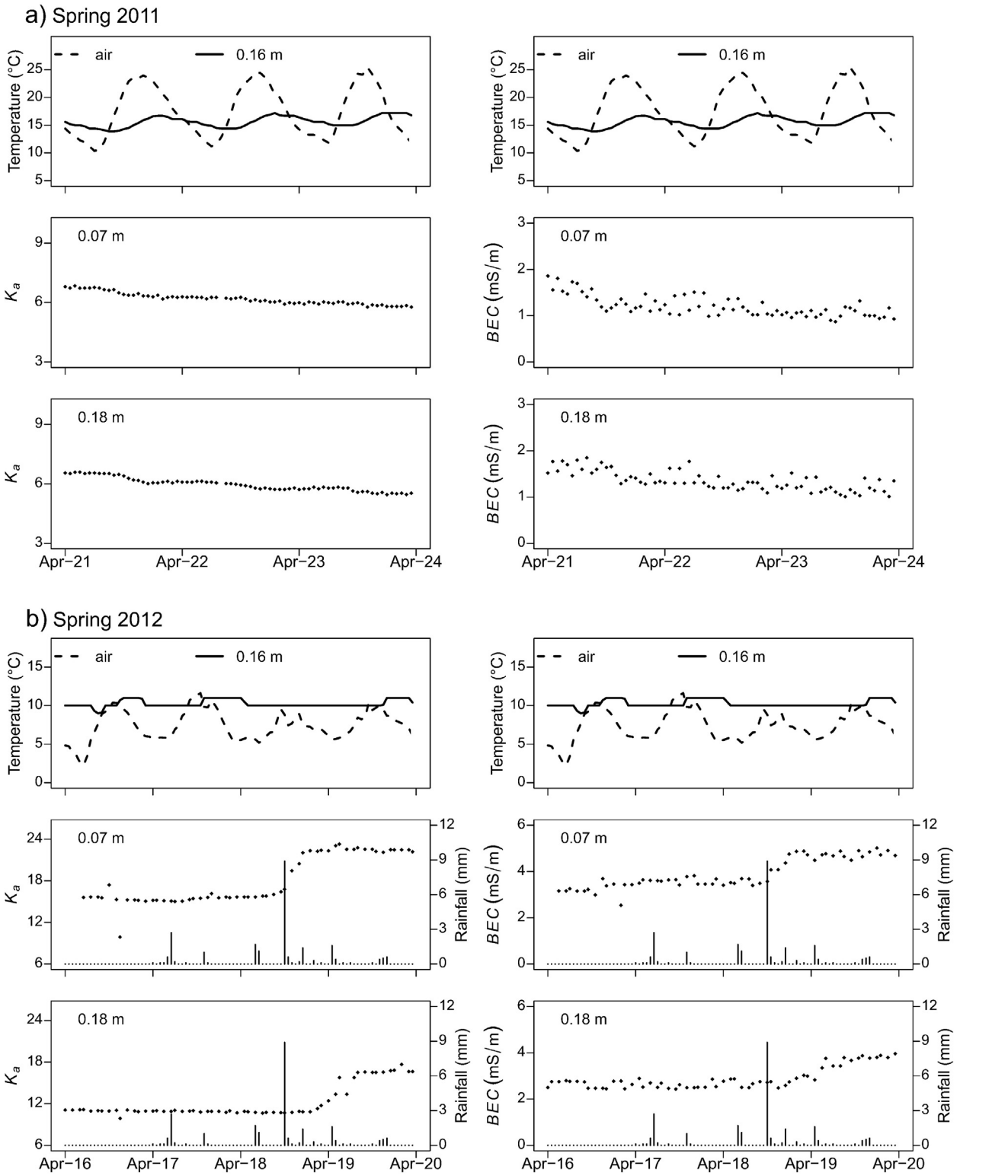

Fig. 6. Daily variation of the EM soil parameters in the topsoil for two selected periods of a) dry and b) wet conditions occurring in Spring 2011 and Spring 2012, respectively.

to precipitation events. It is worth noting that the TDR measurements in this study were not corrected for temperature. The variation of K_a due to temperature was negligible except at very high water contents corresponding to K_a greater than 25, where an additional variability of ± 1 unit of K_a was possible (Curioni, 2013). Rainfall was confirmed to be the dominant driver causing the EM soil properties to change. A time lag of a few hours from a significant rainfall event occurring on the 18th April 2012 and the increase in the values of EM soil properties was recorded by the probes in the topsoil (Fig. 6). Time-domain cross correlation analyses on a number of additional precipitation events confirmed the existence of statistically significant lagged correlations between rainfall and EM soil properties, with lags of the order of several hours up to several days, depending on the depth and on the rainfall intensity, and duration (Curioni, 2013). Although not unexpected, these results have potential implications for planning and interpreting GPR surveys (see Section 4.4).

Both K_a and *BEC* did not show an evident diurnal cycle for the soil studied. The lack of a diurnal cycle for soil water content has been previously reported in the literature for other soil types (Mohanty et al., 1998). It is reasonable to assume that in the absence of a diurnal cycle for temperature it is likely that both K_a and *BEC* do not exhibit a diurnal cyclic variation. This, however, might not be true for locations with highly conductive soils and significant daily temperature variation.

4.3. Impact of seasonal conditions on GPR

The variation of the EM soil properties could have an important impact on the performance of GPR. In order to demonstrate this, extreme wet and dry conditions over the monitoring period were selected and analysed based on the K_a values measured by the TDR probes. At the wet extreme the K_a along the soil profile ranged between approximately 9 and 25, with the majority of probes measuring values greater than 15. At the dry extreme the measured K_a was between approximately 3 and 9, with the majority of probes measuring values smaller than 5. Fig. 7 shows the processed radar sections obtained at these extremes over the buried targets at the test site. The white arrows with white and black tips show the pipes specifically buried for this study (metal and plastic, respectively. See also Fig. 2c); the black arrows indicate the approximate location of other pipes/objects already present on site. The quality of the images was substantially reduced during wet conditions (Fig. 7a and b) as compared to dry conditions (Fig. 7c and d), particularly at 700 MHz, likely because of greater attenuation. The pipes on the right of the section, buried at approximately 1 m depth, were not clearly visible during wet conditions and therefore could potentially remain undetected. The unidentified object on the right of the section, indicated by a black arrow in Fig. 7c and d, was only visible during dry conditions. Despite the low EM loss due to the negligible *BEC*, the abundance of cobbles of the dimension of a few centimetres contributed to dissipate the signal through multiple reflections. Increased scattering due to the presence of cobbles, bricks and other object is a common problem in anthropogenic materials and can significantly reduce the quality of GPR images (Igel, 2008; Slob et al., 2009; Igel et al., 2011).

Table 3 shows the signal propagation velocity (m/ns) and K_a for the wet and dry extremes obtained after fitting the hyperbola generated from the metal pipe at approximately 5 m along the transect and 0.53 m deep (second white arrow from the left in Fig. 7) using the GRED software. This metal pipe was chosen for the analysis because it was always detectable and it could be approximated more realistically to a point source compared to the larger plastic pipe at the same depth. The deeper targets could not be used for this comparison because of the difficulty of fitting the hyperbolae during wet conditions. Due to the non-dispersive nature of the soil, fitting using the two different GPR frequencies returned very similar values of K_a. A velocity variation was observed corresponding to wet and dry conditions, with a mean absolute difference of 0.054 m/ns. The K_a measured with GPR was used in this analysis because it was considered more representative of the bulk soil conditions above the target (i.e. the TDR measurements are more localised).

The variation in velocity at extreme soil conditions has important implications for accurately determining the depth of underground objects. Taking the pipe buried at 0.53 m depth as an example of a target for which the depth is not known and cannot be determined (e.g. a hyperbola cannot be fitted), a K_a value is required in order to estimate the propagation velocity (Eq. (3)) and therefore the target depth. It is

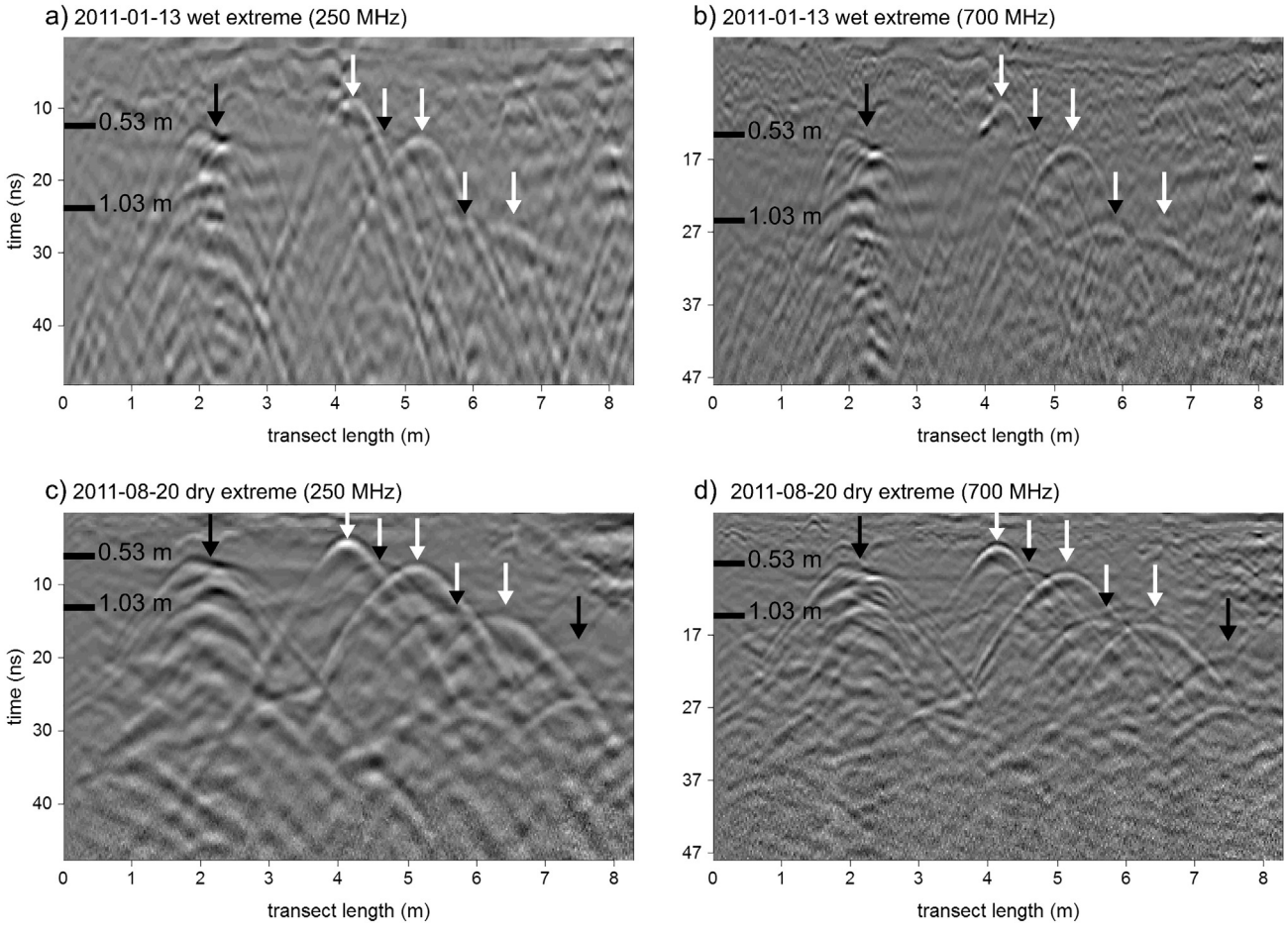

Fig. 7. Radar sections obtained using two different frequencies during a) and b) wet conditions, and during c) and d) dry conditions. [Note: the vertical arrows indicate the approximate position of the buried targets. The plastic pipes are shown in white with a black tip, the metal pipes in white, the pre-existing pipes in black.]

Table 3
Propagation velocity and estimated target depths with relative error calculated using different K_a input values, i.e. the actual K_a measured by GPR using the metal target at 0.53 m, the average K_a measured by TDR over the same depth, and the 'typical' K_a values for the soil studied (Daniels, 2004).

	13-01-2011 Wet conditions Meas. K_a (GPR)	20-08-2011 Dry conditions Meas. K_a (GPR)	13-01-2011 Wet conditions Average K_a (TDR)	20-08-2011 Dry conditions Average K_a (TDR)	13-01-2011 Wet conditions Typical K_a (wet sand)	20-08-2011 Dry conditions Typical K_a (dry sand)
Input K_a	13.4	4.9	9.5	9.5	20.0	4.0
Velocity (m/ns) calculated from Eq. (3)	0.082	0.136	0.097	0.097	0.067	0.150
Time at 0.53 m (ns)	13.00	7.75	13.00	7.75	13.00	7.75
Target depth (m)	0.53	0.53	0.63	0.38	0.44	0.58
Depth error (m)			0.10	0.15	0.10	0.05
Depth error (%)			19.0	28.5	18.0	10.1

of critical importance to estimate a value of K_a accounting for both the soil type and conditions. Table 3 shows the error in depth estimation obtained by using the average K_a corresponding to 0.53 m (i.e. 9.5) measured by the TDR probes and by using typical values for wet and dry sand as reported in the literature (Daniels, 2004). The average value of K_a above 0.53 m was calculated from the TDR probes using the refractive index averaging method (Topp et al., 1982; Robinson et al., 2003), according to Eq. (4).

$$K_{a(TDR)} = \left(\frac{\Sigma L_i \sqrt{K_{a_i}}}{\Sigma L_i}\right)^2 \quad (4)$$

where L_i is the thickness of the soil layer i with contrasting values of K_a compared to the adjacent layers. For this analysis, and a subsequent comparison between TDR and GPR described in Section 4.5, the soil profile was divided into layers of varying thickness down to a depth of 1.08 m (i.e. corresponding to the deepest TDR probe) based on the measured K_a values and the depth of the buried probes. Three layers of thickness 0.10 m, 0.22 m and 0.21 m were used to describe the conditions above 0.53 m.

As mentioned above, different input K_a values were used to calculate the signal velocity using Eq. (3). The K_a obtained from fitting the GPR hyperbola was the correct value as it was an actual measurement representing the soil conditions at the time of the survey (first two columns in Table 3). The average K_a measured by the TDR probes during the entire monitoring period calculated using Eq. (4) was chosen as an arbitrary input K_a (second and third columns in Table 3). Finally, typical K_a values reported in the literature for wet and dry conditions were also used (fourth and fifth columns in Table 3). After converting the input K_a to velocity using Eq. (3), the depth of the target was calculated by multiplying the velocity and the time of the top reflection corresponding to

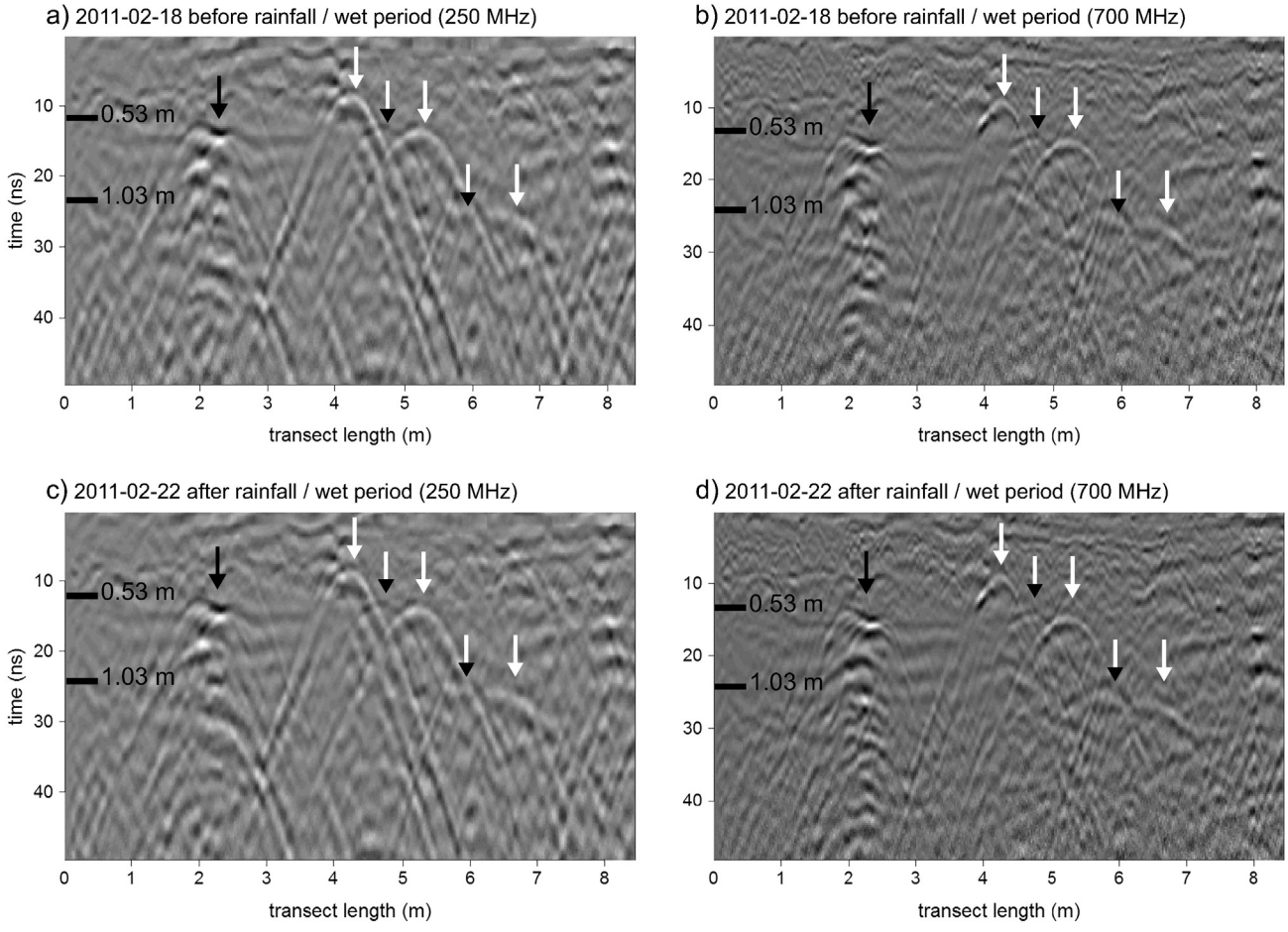

Fig. 8. Radar sections obtained a) and b) before, and c) and d) after a rainfall event occurring during wet soil conditions.

the metal target buried at 0.53 m (second white arrow from the left in Fig. 7). This value was halved to account for the two way travel of the signal. It is apparent that using the average K_a value measured by TDR over the monitoring period produced significant errors of 19% and 28.5% if used during wet and dry conditions, respectively. Daniels (2004) reported values of 10–30 for wet sand and 2–6 for dry sand. These ranges are quite large for wet conditions but help reduce the error of depth estimation, particularly during dry conditions (Table 3). It is therefore important to measure or assess the soil conditions during GPR surveys if more accurate estimations of the target depths are needed, for example during repair/new installation works on sites with a high density of buried utilities and higher risk of strikes.

Comparable errors in depth estimation caused by lateral variations of water content were also reported in the literature (Boll et al., 1996). This demonstrates the importance of both the spatial and temporal variations of the soil K_a for accurate measurements of the target depths. If the soil type is known, an improved estimation of K_a (and therefore depth) can be obtained by using mixing models (Martinez and Byrnes, 2001) or by numerical simulations (Pennock et al., 2012). Alternatively, if the soil volumetric water content can be assessed, a value of K_a can be estimated from petrophysical relationships (e.g. Topp et al., 1980; Birchak et al., 1974). If a probe can be inserted in the ground, technologies such as TDR can be used to provide a direct and therefore more accurate measurement of the soil K_a.

4.4. Impact of rainfall events on GPR

Three significant rainfall events spread over different seasons in 2011 were selected in order to study the impact of rainfall on the GPR results. GPR surveys were conducted before and 3–4 days after these rainfall events. Fig. 8 shows the radar sections obtained during a rainfall event occurring in February 2011 during wet soil conditions. Fig. 9 shows the results of a rainfall event occurring in October 2011 during dry soil conditions. The amount and duration of precipitation were approximately comparable and are shown in Table 4. It is interesting to note that while there was only a minor change in the image quality during the February event (Fig. 8c and d are not dissimilar to Fig. 8a and b), the quality was evidently reduced during the October event (Fig. 9). As compared to the strong targets visible before the rainfall event (Fig. 9a and b), these became less clear afterwards, particularly so at increasing depth and for the plastic pipes (white arrows with a black tip in Fig. 9). The unidentified object indicated by the black arrow on the right of the radar sections in Fig. 9 disappeared after the rainfall event. Analogous results were observed for a similar event occurring in June 2011 during dry conditions. These findings indicate that the ability of detection is not further reduced by rainfall events if the soil conditions are already wet, but there might be implications for surveys following rainfall events during dry conditions. This is a significant finding, as traditionally, wet soils have been perceived as more problematic for GPR surveys. Soil water content heterogeneity is known to be responsible for the deterioration of the GPR signals and was shown to significantly affect the GPR performance on low-conductive sandy soils in other studies (Igel, 2008; Igel et al., 2011). Since the results reported here were based on a limited number of cases it might not be appropriate to extend these conclusions to rainfall events of different intensity and other soil types. However, it is reasonable to assume that if the soil is subject to water infiltration following rainfall it is likely to become less suited to GPR, either because of an increasing signal attenuation, for example in clayey soils, or because of an increase in signal scattering as happened in this study.

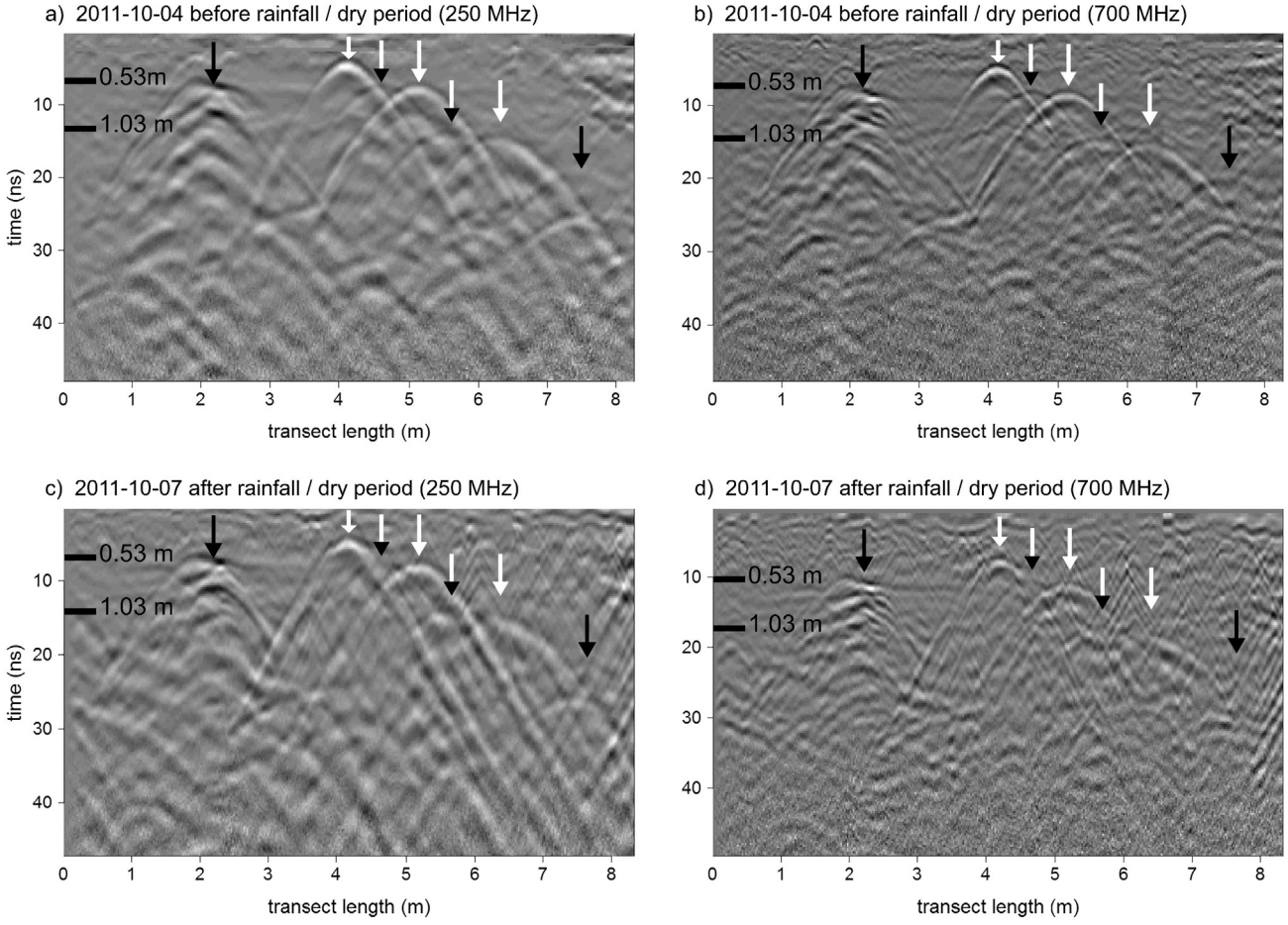

Fig. 9. Radar sections obtained a) and b) before, and c) and d) after a rainfall event occurring during dry soil conditions.

Table 4
Variation of velocity and K_a before and after three significant rainfall events occurring in 2011.

Rainfall event 1 (10.2 mm in 10 h)	18/02/2011	22/02/2011	Difference
Velocity (m/ns)	0.085	0.083	0.002
K_a	12.4	13.6	1.3
Rainfall event 2 (16.8 mm in 20 h)	10/06/2011	14/06/2011	Difference
Velocity (m/ns)	0.120	0.113	0.007
K_a	6.3	7.1	0.8
Rainfall event 3 (8.3 mm in 12 h)	04/10/2011	07/10/2011	Difference
Velocity (m/ns)	0.133	0.125	0.008
K_a	5.1	5.8	0.7

Table 4 shows the variation in velocity and K_a measured by GPR before and after the three selected rainfall events. K_a increased by approximately 1 unit and the propagation velocity of 0.006 m/ns. These values were greater than the uncertainty measured from the repeated GPR scans (i.e. the standard deviations between repeated scans were smaller than 0.001 m/ns and 0.2 for propagation velocity and K_a, respectively). However, they do suggest that the conditions of sandy soils might not change dramatically after single rainfall events and that prolonged wet or dry periods are responsible for the seasonal changes in the soil.

4.5. Comparison between TDR and GPR

By fitting the hyperbolae of the metal pipes buried at 0.32 m, 0.53 m and 1.03 m it was possible to compare the average K_a above the pipes measured by GPR with both frequencies (i.e. 250 MHz and 700 MHz) and the average K_a corresponding to the same depths measured by the TDR probes using Eq. (4). Ten datasets spanning across the seasons were used comprising the wet/dry extremes and rainfall events described above, and warm/cold extremes occurring on 28 July 2011 and 08 February 2012, respectively (Fig. 10). The K_a values measured by GPR at the two different frequencies were very similar (Fig. 10) and their mean value was used for comparison with the TDR measurements. A number of measurements from GPR were missing for the deeper pipe because hyperbolae were not clearly visible during wet conditions. In general, GPR and TDR provided analogous measurements of K_a, with a mean absolute difference of 1.41. However, GPR typically measured lower K_a values during wet conditions, for K_a greater than 10. Conversely, it measured higher values for K_a smaller than 10, corresponding to dry conditions. It should be noted that GPR measured a bulk K_a over a large sample of soil, whereas the TDR measurements were limited to the dimensions of the probes, which could only be inserted in pockets of soils containing particles smaller than the separation between the rods. The soil studied contained significant amounts of cobbles that could not be investigated by the TDR probes. As rocks have a very low K_a this could explain why the bulk K_a measured by the GPR (i.e. containing the cobbles) was lower than the K_a measured by TDR during wet conditions. However, the GPR measured higher values than TDR during dry conditions (see the Summer months in Fig. 10). It was noted that the TDR probes in the topsoil did not respond to rainfall events during the Summer months and did not measure an increase in K_a and *BEC* following rainfall events as compared to the other seasons. The soil might have cracked and become hydrophobic during dry conditions leaving more air in the pores close to the TDR probes and explaining the lower K_a values measured by TDR. These air gaps either allowed for very quick drainage or the particles surrounding them became hydrophobic and impeded the flow of water in the volume measured by the TDR probes. This phenomenon stopped in the Autumn when the conditions became wetter again. Notwithstanding this, the differences measured were relatively small and confirmed that both TDR and GPR can be used for measuring K_a soil profiles either by inserting TDR probes at multiple depths or by fitting clear hyperbolae detected by GPR. It is interesting to note that the differences between TDR and GPR were greater if other means of averaging the TDR probes

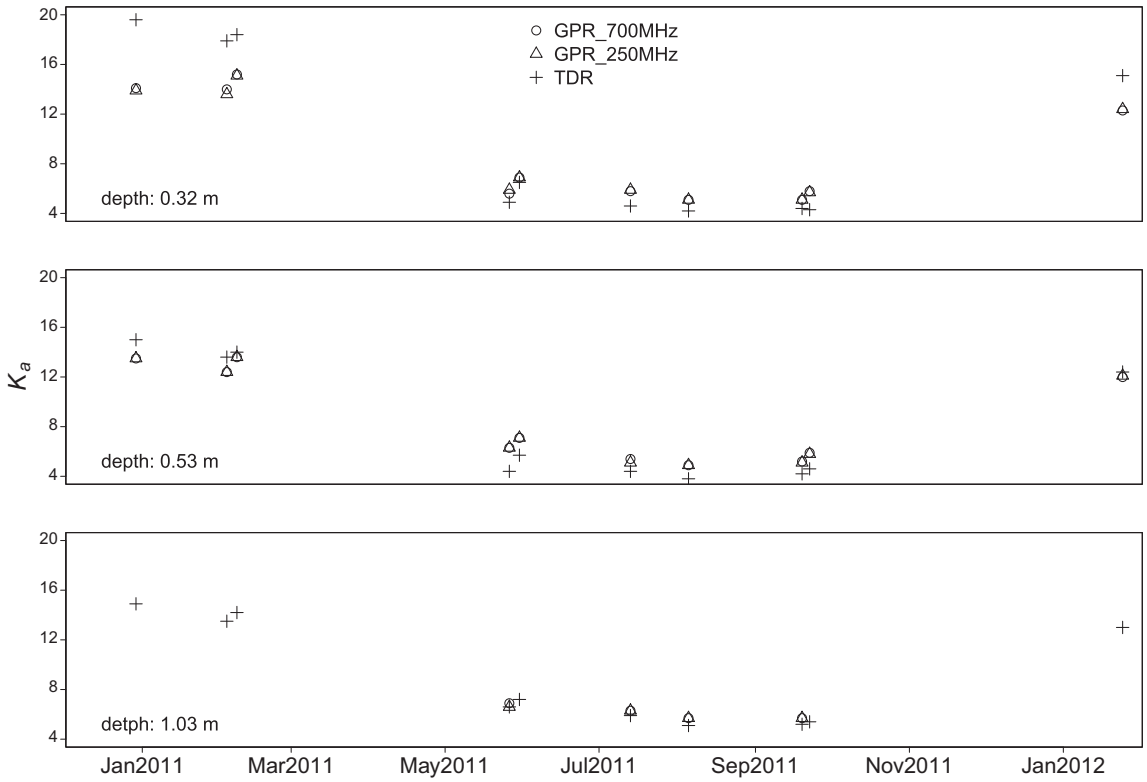

Fig. 10. K_a values measured with GPR and TDR for a number of selected dates comprising wet/dry extremes, warm/cold extremes and rainfall events.

other than the refractive index method (Eq. (4)) were used. As mentioned earlier, the soil profile was divided into six layers of different thickness based on their K_a values and their depths. If using simple arithmetic or weighted K_a average by layer thickness the mean absolute difference increased to 1.91 and 1.49, respectively. Similarly, using fewer layers increased the difference between TDR and GPR measurements. Due to the high spatial variability in the topsoil and due to the relatively small number of probes installed in the top 0.3 m the differences between TDR and GPR were greater when compared over this depth (Fig. 10). The differences became smaller at greater depths, demonstrating the ability of multiple TDR probes buried at different depths to provide an average characterisation of the EM behaviour of the soil that can be directly used for GPR applications.

GPR was able to measure slightly different values of K_a depending on which hyperbola was used for the fitting (i.e. from different targets at different depths) indicating that it could be used for measuring vertical gradients of K_a in the presence of clear targets at different depths.

5. Conclusions

This paper has described a unique study to monitor the EM properties (K_a and *BEC*) of an anthropogenic sandy soil in a long-term field trial (Aug 2010–Jul 2012) using TDR up to a depth of 1 m in order to determine the extent of their variation and their impact on GPR results, particularly depth, for the purpose of utility detection. During the monitored period a wide range of weather conditions occurred, and, importantly, the obtained high quality data set fills in a gap in the literature with respect to long-term monitoring over several seasons using TDR and GPR alongside each other. The results will benefit utility surveyors by providing a better understanding of the impact of weather on GPR performance and depth determination of buried utilities, and therefore giving GPR practitioners useful information for selecting the best equipment, providing better confidence in the data (including depth) and ultimately leading to an improved 3D representation of the subsurface. It is important to point out that the findings presented in this paper were obtained on a sandy soil and therefore the results might not apply to soils with considerable amounts of clay.

It was found that the soil K_a varied significantly with the seasons following prolonged periods of dry and wet conditions, with extreme values of 3.7 and 25.6 for the topsoil and 5.6 and 15.8 for the bulk subsoil. The corresponding velocity variation at these extremes was 0.098 m/ns and 0.054 m/ns for the topsoil and bulk subsoil, respectively. Due to the sandy and gravelly nature of the soil studied, *BEC* showed smaller variability, with extremes of 0.1 and 10.5 mS/m for the topsoil and 1.0 and 8.2 mS/m for the bulk subsoil. The soil also showed some variability with depth in these parameters, with less variability during dry periods. The soil EM properties were primarily affected by changes in the soil water content caused by prolonged rainfall and evaporation events and did not show a diurnal variation cycle.

Importantly, it was confirmed that the temporal variation of the EM soil properties affects GPR performance, with degradation of the GPR images during wet periods and a few days after significant rainfall events following dry periods. Another key finding demonstrated in the paper is that using arbitrary average values of K_a and *BEC* as inputs can lead to significant inaccuracies in the estimation of the depth of buried features, with errors potentially up to approximately 30% over a depth of 0.50 m. These inaccuracies can have major consequences for utility detection and subsequent streetworks that are relying on having as accurate depth information as possible.

Whenever a hyperbola cannot be fitted it is recommended that the soil conditions are measured or assessed during GPR surveys, and if this is not possible to use typical wet and dry K_a values reported in the literature for the soil studied for improved estimations of the target depths. Finally, a comparison between the TDR and GPR results showed some interesting differences probably due to the different volumes of soil sampled by the two methods. Overall it can be concluded that both techniques can be used to measure K_a soil profiles either by inserting TDR probes at multiple depths or by fitting clear hyperbolae detected by GPR.

Acknowledgements

The authors wish to thank the UK Engineering and Physical Sciences Research Council (EPSRC) for funding the research that underpinned this study via EPSRC Grants EP/F065965, EP/F06585X, EP/F065906, EP/F065973 and EP/F06599X.

References

ASCE, 2002. Standard Guideline for the Collection and Depiction of Existing Subsurface Utility Data (No. CI/ASCE 38-02). American Society of Civil Engineers, Reston, VA, USA.

Bechtold, M., Huisman, J.A., Weihermüller, L., Vereecken, H., 2010. Accurate determination of the bulk electrical conductivity with the TDR100 cable tester. Soil Sci. Soc. Am. J. 74: 495–501. http://dx.doi.org/10.2136/sssaj2009.0247.

Birchak, J., Gardner, C., Hipp, J., Victor, J., 1974. High dielectric-constant microwave probes for sensing soil-moisture. Proc. IEEE 62:93–98. http://dx.doi.org/10.1109/PROC.1974.9388.

Bittelli, M., Salvatorelli, F., Pisa, P.R., 2008. Correction of TDR-based soil water content measurements in conductive soils. Geoderma 143:133–142. http://dx.doi.org/10.1016/j.geoderma.2007.10.022.

Bobylev, N., 2016. Underground space as an urban indicator: measuring use of subsurface. Tunn. Undergr. Space Technol. 55:40–51. http://dx.doi.org/10.1016/j.tust.2015.10.024.

Boll, J., Van Rijn, R.P.G., Weiler, K.W., Ewen, J.A., Daliparthy, J., Herbert, S.J., Steenhuis, T.S., 1996. Using ground-penetrating radar to detect layers in a sandy field soil. Geoderma 70, 117–132.

BSI, 1999. Methods of test for soils for civil engineering purposes. Classification tests. BS 1377-2. British Standards Institution, London, UK.

BSI, 2014. Specification for Underground Utility Detection, Verification and Location (No. PAS 128:2014). British Standards Institution, London, UK.

BSI, 2015. Code of practice for site investigations. BS5930. British Standards Institution, London, UK.

Cassidy, N.J., 2008. Frequency-dependent attenuation and velocity characteristics of nano-to-micro scale, lossy, magnetite-rich materials. Near. Surf. Geophys. 6, 341–354.

Cassidy, N.J., 2009. Electrical and magnetic properties of rocks, soils and fluids. In: Jol, H. (Ed.), Ground Penetrating Radar Theory and Applications. Elsevier Science & Technology, Oxford, UK, pp. 41–72.

Curioni, G., 2013. Investigating the Seasonal Variability of Electromagnetic Soil Properties Using Field Monitoring Data from Time-Domain Reflectometry Probes. (Ph.D. Thesis). University of Birmingham.

Curioni, G., Chapman, D.N., Metje, N., Foo, K.Y., Cross, J.D., 2012. Construction and calibration of a field TDR monitoring station. Near. Surf. Geophys. 10, 249–261.

Daniels, D.J., 2004. Ground Penetrating Radar. second ed IET, London, UK.

Doolittle, J.A., Collins, M.E., 1995. Use of soil information to determine application of ground penetrating radar. J. Appl. Geophys. 33:101–108. http://dx.doi.org/10.1016/0926-9851(95)90033-0.

Doolittle, J.A., Minzenmayer, F.E., Waltman, S.W., Benham, E.C., Tuttle, J.W., Peaslee, S.D., 2007. Ground-penetrating radar soil suitability map of the conterminous United States. Geoderma 141:416–421. http://dx.doi.org/10.1016/j.geoderma.2007.05.015.

Ferré, P.A., Knight, J.H., Rudolph, D.L., Kachanoski, R.G., 1998. The sample areas of conventional and alternative time domain reflectometry probes. Water Resour. Res. 34: 2971–2979. http://dx.doi.org/10.1029/98WR02093.

Foo, K.Y., Hao, T., Curioni, G., Chapman, D.N., Metje, N., Atkins, P.R., 2011. A knowledge-based system for evaluating the impact of soil properties on the performance of utility location technologies: design and case study. Presented at the ICPTT 2011: Sustainable Solutions for Water, Sewer, Gas, and Oil Pipelines - Proceedings of the International Conference on Pipelines and Trenchless Technology 2011:pp. 810–825 http://dx.doi.org/10.1061/41202(423)87.

Gong, Y.S., Cao, Q.H., Sun, Z.J., 2003. The effects of soil bulk density, clay content and temperature on soil water content measurement using time-domain reflectometry. Hydrol. Process. 17:3601–3614. http://dx.doi.org/10.1002/hyp.1358.

Hatzichristodulu, V.C., Baker, R.D., Tellam, J.H., 2002. High Resolution Electrical Monitoring of Fluid Flow Through the Unsaturated Zone (R&D Technical Report P2-042/TR1 No. R&D Technical Report P2-042/TR1). Environment Agency.

Heimovaara, T.J., Bouten, W., 1990. A computer-controlled 36-channel time domain reflectometry system for monitoring soil water contents. Water Resour. Res. 26: 2311–2316. http://dx.doi.org/10.1029/WR026i010p02311.

Herkelrath, W., Hamburg, S., Murphy, F., 1991. Automatic, Real-Time Monitoring of Soil-Moisture in a Remote Field Area with Time Domain Reflectometry. Water Resour. Res. 27:857–864. http://dx.doi.org/10.1029/91WR00311.

Herkelrath, W.N., Delin, G.N., 2001. Long-term monitoring of soil-moisture in a harsh climate using reflectometer and TDR probes. In: Dowding, C.H. (Ed.), Proceedings of the Second International Symposium and Workshop on Time Domain Reflectometry for Innovative Geotechnical Applications. Presented at the Second International Symposium and Workshop on Time Domain Reflectometry for Innovative Geotechnical Applications. Northwestern University, Infrastructure Technology Institute, Evanston, IL, pp. 262–272.

Huisman, J.A., Sperl, C., Bouten, W., Verstraten, J.M., 2001. Soil water content measurements at different scales: accuracy of time domain reflectometry and ground-penetrating radar. J. Hydrol. 245:48–58. http://dx.doi.org/10.1016/S0022-1694(01)00336-5.

Huisman, J.A., Hubbard, S.S., Redman, J.D., Annan, A.P., 2003a. Measuring soil water content with ground penetrating radar: a review. Vadose Zone J. 2, 476–491.
Huisman, J.A., Snepvangers, J.J.J.C., Bouten, W., Heuvelink, G.B.M., 2003b. Monitoring temporal development of spatial soil water content variation: comparison of ground penetrating radar and time domain reflectometry. Vadose Zone J. 2, 519–529.
Huisman, J.A., Lin, C.P., Weihermüller, L., Vereecken, H., 2008. Accuracy of bulk electrical conductivity measurements with time domain reflectometry. Vadose Zone J. 7: 426–433. http://dx.doi.org/10.2136/vzj2007.0139.
Igel, J., 2008. The small-scale variability of electrical soil properties – influence on GPR measurements. Proc. 12th International Conference on Ground Penetrating Radar. Presented at the 12th International Conference on Ground Penetrating Radar, Birmingham, UK.
Igel, J., Takahashi, K., Preets, H., 2011. Electromagnetic soil properties and performance of GPR for landmine detection: how to measure, how to analyse and how to classify? Proc. 6th International Workshop on Advanced Ground Penetrating Radar (IWAGPR). Presented at the 6th International Workshop on Advanced Ground Penetrating Radar (IWAGPR), Aachen, Germany
Kowalsky, M.B., Dietrich, P., Teutsch, G., Rubin, Y., 2001. Forward modeling of ground-penetrating radar data using digitized outcrop images and multiple scenarios of water saturation. Water Resour. Res. 37:1615–1625. http://dx.doi.org/10.1029/2001WR900015.
Lin, C.-P., Chung, C.-C., Tang, S.-H., 2007. Accurate time domain reflectometry measurement of electrical conductivity accounting for cable resistance and recording time. Soil Sci. Soc. Am. J. 71:1278–1287. http://dx.doi.org/10.2136/sssaj2006.0383.
Lin, C.-P., Chung, C.-C., Huisman, J.A., Tang, S.-H., 2008. Clarification and calibration of reflection coefficient for electrical conductivity measurement by time domain reflectometry. Soil Sci. Soc. Am. J. 72:1033–1040. http://dx.doi.org/10.2136/sssaj2007.0185.
Logsdon, S., 2005. Time domain reflectometry range of accuracy for high surface area soils. Vadose Zone J. 4:1011–1019. http://dx.doi.org/10.2136/vzj2004.0108.
Lunt, I.A., Hubbard, S.S., Rubin, Y., 2005. Soil moisture content estimation using ground-penetrating radar reflection data. J. Hydrol. 307:254–269. http://dx.doi.org/10.1016/j.jhydrol.2004.10.014.
Martinez, A., Byrnes, A.P., 2001. Modeling dielectric-constant values of geologic materials: an aid to ground-penetrating radar data collection and interpretation. Curr. Res. Earth Sci. 247, 1–16.
Menziani, M., Pugnaghi, S., Vincenzi, S., Santangelo, R., 2003. Soil moisture monitoring in the Toce valley (Italy). Hydrol. Earth Syst. Sci. 7, 890–902.
Metje, N., Crossland, S.M., Ahmad, B., 2015. Causes, impacts and costs of strikes on buried utility assets. Proc. ICE – Munic. Eng. 168:165–174. http://dx.doi.org/10.1680/muen.14.00035.
Mohanty, B.P., Shouse, P.J., Van, G., 1998. Spatio-temporal dynamics of water and heat in a field soil. Soil Tillage Res. 47:133–143. http://dx.doi.org/10.1016/S0167-1987(98)00084-1.
Pennock, S.R., Jenks, C.H.J., Orlando, G., Redfern, M.A., 2012. In-pipe GPR configuration and the determination of target depth and ground permittivity. Presented at the International Geoscience and Remote Sensing Symposium (IGARSS):pp. 618–621 http://dx.doi.org/10.1109/IGARSS.2012.6351518.
Rajeev, P., Chan, D., Kodikara, J., 2012. Ground-atmosphere interaction modelling for long-term prediction of soil moisture and temperature. Can. Geotech. J. 49:1059–1073. http://dx.doi.org/10.1139/T2012-068.
Rajkai, K., Ryden, B., 1992. Measuring areal soil-moisture distribution with the TDR method. Geoderma 52:73–85. http://dx.doi.org/10.1016/0016-7061(92)90076-J.
Read, G.F., Vickridge, I., 2004. Social or indirect costs of public utility works. Sewers: Replacement and New Construction. Elsevier Ltd, pp. 339–366.
Robinson, D.A., Jones, S.B., Wraith, J.M., Or, D., Friedman, S.P., 2003. A review of advances in dielectric and electrical conductivity measurement in soils using time domain reflectometry. Vadose Zone J. 2, 444–475.
Rogers, C.D.F., 2015. Assessing the underworld - remote sensing to support smart and liveable cities. 2015 8th International Workshop on Advanced Ground Penetrating Radar (IWAGPR). Presented at the 2015 8th International Workshop on Advanced Ground Penetrating Radar (IWAGPR):pp. 1–4 http://dx.doi.org/10.1109/IWAGPR.2015.7292634.
Rogers, C.D.F., Chapman, D.N., Entwisle, D., Jones, L., Kessler, H., Metje, N., Mica, L., Morey, M., Pospil, P., Price, S., Raclavsky, J., Raines, M., Scott, H., Thomas, A.M., 2009. Predictive mapping of soil geophysical properties for GPR utility location surveys. 5th International Workshop on Advanced Ground Penetrating Radar. Presented at the 5th International Workshop on Advanced Ground Penetrating Radar, Granada, Spain.
Saarenketo, T., 1998. Electrical properties of water in clay and silty soils. J. Appl. Geophys. 40:73–88. http://dx.doi.org/10.1016/S0926-9851(98)00017-2.
Slob, E., Liu, F., Pospisil, P., Mica, L., 2009. Seasonal changes of soil geophysical properties, with applications to GPR utility location surveys. Proc. 5th International Workshop on Advanced Ground Penetrating Radar. Presented at the 5th International Workshop on Advanced Ground Penetrating Radar, Granada, Spain.
Thomas, A.M., Chapman, D.N., Rogers, C.D.F., Metje, N., Atkins, P.R., Lim, H.M., 2008. Broadband apparent permittivity measurement in dispersive soils using quarter-wavelength analysis. Soil Sci. Soc. Am. J. 72:1401–1409. http://dx.doi.org/10.2136/sssaj2007.0319.
Thomas, A.M., Rogers, C.D.F., Chapman, D.N., Metje, N., Castle, J., 2009. Stakeholder needs for ground penetrating radar utility location. J. Appl. Geophys. 67:345–351. http://dx.doi.org/10.1016/j.jappgeo.2008.07.006.
Thomas, A.M., Chapman, D.N., Rogers, C.D.F., Metje, N., 2010a. Electromagnetic properties of the ground: part I - fine-grained soils at the Liquid Limit. Tunn. Undergr. Space Technol. 25:714–722. http://dx.doi.org/10.1016/j.tust.2009.12.002.
Thomas, A.M., Chapman, D.N., Rogers, C.D.F., Metje, N., 2010b. Electromagnetic properties of the ground: part II - the properties of two selected fine-grained soils. Tunn. Undergr. Space Technol. 25:723–730. http://dx.doi.org/10.1016/j.tust.2009.12.003.
Thring, L.M., Boddice, D., Metje, N., Curioni, G., Chapman, D.N., Pring, L., 2014. Factors affecting soil permittivity and proposals to obtain gravimetric water content from time domain reflectometry measurements. Can. Geotech. J. 51:1303–1317. http://dx.doi.org/10.1139/cgj-2013-0313.
Topp, G.C., Davis, J.L., Annan, A.P., 1980. Electromagnetic determination of soil water content: measurements in coaxial transmission lines. Water Resour. Res. 16: 574–582. http://dx.doi.org/10.1029/WR016i003p00574.
Topp, G., Davis, J., Annan, A., 1982. Electromagnetic determination of soil-water content using TDR .1. Applications to wetting fronts and steep gradients. Soil Sci. Soc. Am. J. 46, 672–678.
Topp, G.C., Zegelin, S., White, I., 2000. Impacts of the real and imaginary components of relative permittivity on time domain reflectometry measurements in soils. Soil Sci. Soc. Am. J. 64, 1244–1252.
Weiler, K.W., Steenhuis, T.S., Boll, J., Kung, K.-J.S., 1998. Comparison of ground penetrating radar and time-domain reflectometry as soil water sensors. Soil Sci. Soc. Am. J. 62, 1237–1239.
Zhang, J., Lin, H., Doolittle, J., 2014. Soil layering and preferential flow impacts on seasonal changes of GPR signals in two contrasting soils. Geoderma 213:560–569. http://dx.doi.org/10.1016/j.geoderma.2013.08.035.